Contribution from the Chemistry Departments, The University, Leicester LE1 7RH, U.K., and McMaster University, Hamilton, Ontario L8S 4M1, Canada

Crystal Structure of $Cs^+[(XeOF_4)_3F]^-$ and Vibrational Study of the ^{18}O-Enriched $[XeOF_5]^-$ and $[(XeOF_4)_3F]^-$ Anions

JOHN H. HOLLOWAY,*[1] VENCESLAV KAUČIČ,[1] DOMINIQUE MARTIN-ROVET,[2] DAVID R. RUSSELL,[1] GARY J. SCHROBILGEN,*[3] and HENRY SELIG[1]

Received February 28, 1984

The cesium salts of the anions $[XeOF_5]^-$ and $[(XeOF_4)_3F]^-$ have been prepared and characterized. The Raman spectra of $Xe^{16}OF_5^-$ and $Xe^{18}OF_5^-$ are consistent with a stereochemically active lone pair in the xenon valence shell that results in a distorted octahedral arrangement of five fluorines and one oxygen around xenon to give C_s symmetry. The X-ray structure of $Cs^+[(XeOF_4)_3F]^-$ has been obtained. Crystals are cubic, space group $Pa3$ with a = 13.933 (7) Å and Z = 8. The structure was solved by means of Patterson and Fourier syntheses and refined by the least-squares method to R = 0.0969 and R_w = 0.0960 for 355 reflections. The anion possesses C_3 symmetry and consists of octahedra of O=XeF_4E (E = lone electron pair; mean Xe-F = 1.90 (3) Å; Xe=O = 1.70 (5) Å) linked through three fluorine bridges (Xe---F = 2.62 (1) Å, ∠(Xe---F---Xe) = 116.5 (8)°) with the trigonally bonded fluorine positioned 0.49 Å above the plane defined by the three xenon atoms. The Raman spectra of the $^{16}O/^{18}O$ isotopic isomers of $[(XeOF_4)_3F]^-$ and their associated coupling patterns have been interpreted on the basis of the X-ray structure.

Introduction

The fluoride ion donor abilities of noble-gas fluorides are well established and have resulted in the preparation of oxyfluoro and fluoro cations of xenon and krypton that have been studied in considerable detail.[4-7] With a few notable exceptions, the fluoride ion acceptor properties of noble-gas fluorides and oxyfluorides are less well documented. Only xenon compounds in their +4 and +6 oxidation states have been shown to exhibit fluoride ion-acceptor properties. Xenon(IV) has only one representative in the form of the $[XeOF_3]^-$ anion.[8] In contrast, xenon(VI) compounds, i.e. XeF_6, XeO_3, XeO_2F_2, and $XeOF_4$, possess a diverse fluoride ion-acceptor chemistry. The single-crystal X-ray structures of $[XeF_8]^{2-}$[9] and $[XeO_3F]^-$[10] have been published. A stable $[XeO_2F_3]^-$ anion, resulting from disproportionation of $XeOF_2$ in the presence of CsF, has also been characterized.[8] Complexes of $XeOF_4$ with alkali-metal fluorides and NOF of unspecified structures were first reported by Selig and Moody[11] who isolated $NOF\cdot XeOF_4$ and by Selig[12] who also isolated complexes corresponding to the stoichiometries $CsF\cdot XeOF_4$, $3RbF\cdot 2XeOF_4$, and $3KF\cdot XeOF_4$. More recently, vibrational studies of ^{18}O-enriched preparations of $CsF\cdot XeOF_4$ and $3CsF\cdot XeOF_4$ and X-ray powder diffraction studies of $CsF\cdot 3XeOF_4$ have established the existence of the corresponding novel $[XeOF_5]^-$ and $[(XeOF_4)_3F]^-$ anions.[13] Like the isoelectronic monomer XeF_6, the $[XeOF_5]^-$ anion structure is based upon an octahedron possessing a stereochemically active lone pair of electrons in the xenon valence shell.

The $^{16}O/^{18}O$ isotopic splitting patterns and powder diffraction studies for $Cs^+[(XeOF_4)_3F]^-$ were consistent with a trigonal arrangement of three equivalent $XeOF_4$ molecules coordinated to a central F^- ion. Again, the lone pair in each xenon valence shell was presumed to be stereochemically active.

In the present paper, we report in detail the vibrational spectra of $[XeOF_5]^-$ and $[(XeOF_4)_3F]^-$ and the single-crystal X-ray structure of the novel $[(XeOF_4)_3F]^-$ anion.

Results and Discussion

$Cs^+[XeOF_5]^-$. On the basis of Raman spectroscopic results, $CsF\cdot XeOF_4$ is best formulated as the salt, $Cs^+[XeOF_5]^-$. The anticipated stereochemical activity of the xenon valence shell lone pair should lead to an anion structure (I) that is distorted from

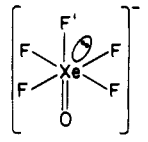

I

C_{4v} symmetry for a pseudooctahedral species to C_s symmetry. Because of the greater stereochemical requirement of a Xe=O bond, the lone pair of the distorted $[XeOF_5]^-$ anion will presumably occupy the octahedral faces adjacent to the axial fluorine.

Under C_{4v} symmetry, $[XeOF_5]^-$ exhibits 11 Raman-active bands (Γ = 4 A_1 + 2 B_1 + B_2 + 4 E) while the distorted C_s structure (I) yields 15 Raman-active bands (Γ = 9 A' + 6 A'') (Figure 1). The vibrational data support the C_s structure for $[XeOF_5]^-$ and have been assigned accordingly by comparison with IOF_5[14] and $[TeOF_5]^-$[15] (C_{4v}) (Table I). The E modes (C_{4v} symmetry) are split into their A' and A'' components under C_s symmetry in $[XeOF_5]^-$. Isotopic enrichment with ^{18}O led to the observation of a total of four groupings of $^{18}O/^{16}O$-dependent bands, three of which are bends and are split into their A' and A'' components under C_s symmetry and these have, accordingly, been assigned to the various modes involving motions of oxygen. The Xe=^{16}O stretch ($^{18}O/^{16}O$ isotopic shift 44 cm^{-1}), which occurs at 883 cm^{-1}, and the Xe—F stretching modes are considerably lower in frequency than the corresponding stretches in either of the neutral molecules, IOF_5[14] and $XeOF_4$,[16] and this is consistent with anion formation.

The Xe-F stretching modes of $[XeOF_5]^-$ lie at much lower frequencies than may have been anticipated, ranging from 420 cm^{-1} for the axial fluorine–xenon (Xe–F') stretch to 544 cm^{-1} for the out-of-phase symmetric XeF_4 stretch, while the corresponding frequencies for the closely related $[TeOF_5]^-$[15] anion are assigned to bands at 581 and 664 cm^{-1}. In contrast, the Te=O stretch (863 cm^{-1}) is found to occur at lower frequency than that of $[XeOF_5]^-$. The effective reduction in stretching force constant for Xe—F stretches appears to be a consequence of localization of the lone electron pair on the faces adjacent to F' (structure I).

(1) The University, Leicester.
(2) Département de Physico-Chimie, Centre d'Etudes Nucléaires de Saclay, 91191 Gif-sur-Yvette, France.
(3) McMaster University.
(4) Bartlett, N.; Sladky, F. O. In "Comprehensive Inorganic Chemistry"; Trotman-Dickenson, A. F., Ed.; Pergamon Press: Oxford, 1973; Vol. 1, Chapter 6.
(5) Gillespie, R. J.; Schrobilgen, G. J. *Inorg. Chem.* **1974**, *13*, 2370.
(6) Boldrini, P.; Gillespie, R. J.; Ireland, P.; Schrobilgen, G. J. *Inorg. Chem.* **1974**, *13*, 1690.
(7) Gillespie, R. J.; Schrobilgen, G. J. *Inorg. Chem.* **1976**, *15*, 22.
(8) Gillespie, R. J.; Schrobilgen, G. J. *J. Chem. Soc., Chem. Commun.* **1977**, 595.
(9) Peterson, S. W.; Holloway, J. H.; Coyle, B. A.; Williams, J. M. *Science* (Washington, D.C.) **1971**, *No. 173*, 1238.
(10) Hodgson, D. J.; Ibers, J. A. *Inorg. Chem.* **1969**, *8*, 326.
(11) Moody, G. J.; Selig, H. *Inorg. Nucl. Chem. Lett.* **1966**, *2*, 319.
(12) Selig, H. *Inorg. Chem.* **1966**, *5*, 183.
(13) Schrobilgen, G. J.; Martin-Rovet, D.; Charpin, P.; Lance, M. *J. Chem. Soc., Chem. Commun.* **1980**, 894.
(14) Holloway, J. H.; Selig, H.; Claassen, H. H. *J. Chem. Phys.* **1971**, *54*, 4305.
(15) Mayer, E.; Sladky, F. *Inorg. Chem.* **1975**, *14*, 589.
(16) de Waard, H.; Bukshpan, S.; Schrobilgen, G. J.; Holloway, J. H.; Martin, D. *J. Chem. Phys.* **1979**, *70*, 3247.

0020-1669/85/1324-0678$01.50/0

Table I. Raman Spectra and Assignments for $XeOF_5^-$ and Related Species

Raman freq,[a] cm^{-1}			
$[XeOF_5]^-$	IOF_5[b]	$TeOF_5^-$[c]	assgnt and approx descrip, C_{4v} sym
883 (66)[d]	927 s	863 s	a_1, ν(X=O)
544 sh	710 w	664 sh	b_1, $\nu_{sym}(XF_4)$ out-of-phase
524 (100)	680 vs	650 vs	a_1, $\nu_{sym}(XF_4)$
473 (34), 468 (29), 435 (12)[e]	647 s	637 vs[n]	e, $\nu_{asym}(XF_4)$
420 (10)	640 vs	581 m	a_1, $\nu(XF')$
410 (7), 396 (24)[e,f]	372 m	347 w	e, $\delta(F'XF_4)$, F'–X=O bend
390 (40)	363 m[h]		b_2, $\delta_{sym}(XF_4)$ out-of-plane
361 (17)	330 w	327 m	a_1, $\delta_{sym}(XF_4)$ in-plane
384 (18), 365 (15)[e,g]	341 s	282 w	e, $\delta(O{=}XF_4)$, OF_3 scissoring
293 (13), 274 (8)[e,h]	307 m		e, $\delta_{asym}(XF_4)$ in-plane, OF_3 puckering
177 (1)	205 vw		b_1, $\delta_{asym}(XF_4)$ out-of-plane
153 (4), 116 (6), 102 (11), 89 (13), 76 (6)			lattice modes

[a] Spectra were recorded from the 5145-Å exciting line of an argon ion laser; Raman shifts are accurate to ±1 cm^{-1}. All data quoted are for the ^{16}O compounds, $^{16}O/^{18}O$ isotopic shifts are given in subsequent footnotes to the table. [b] Reference 14. [c] Reference 15. [d] $^{16}O/^{18}O$ isotopic shift: 44 cm^{-1}. [e] The e mode (C_{4v} symmetry) is split into its a' and a'' components under C_s symmetry. [f] $^{16}O/^{18}O$ isotopic shifts: 3 and 6 cm^{-1} for the 410- and 396-cm^{-1} lines, respectively. [g] $^{16}O/^{18}O$ isotopic shifts: 6 and 13 cm^{-1} for the 384- and 365-cm^{-1} lines, respectively. [h] $^{16}O/^{18}O$ isotopic shifts: 3 and 7 cm^{-1} for the 293- and 274-cm^{-1} lines, respectively.

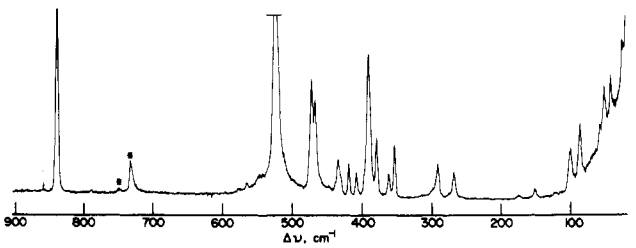

Figure 1. Raman spectrum of 99% ^{18}O-enriched $Cs^+[XeOF_5]^-$ recorded at −196 °C (asterisks denote FEP sample vessel lines).

The proximity of the fluorine bond pairs to the electron lone pair, and the ensuing bond pair–lone pair repulsions, would be expected to lower their respective stretching force constants. If the electron lone pair is localized on one octahedral face (on the vibrational time scale), the repulsive interactions with the two adjacent equatorial fluorine atoms would also be expected to modify the frequencies of the two nonadjacent equatorial fluorines that are vibrationally strongly coupled to the adjacent pair of equatorial fluorines. The opposite influence is anticipated for the Xe–O stretch, which should increase in frequency relative to that in the C_{4v} alternative. This is presumed to arise from the longer, more ionic Xe—F bonds that result from repulsive interactions with the electron lone pair. In this context, it is interesting to note that the Xe=O stretching frequency is in fact higher than that in the $[TeOF_5]^-$ anion, which possesses no lone pair in the tellurium valence shell.

The three remaining low-frequency pairs of $^{18}O/^{16}O$-dependent bands have been assigned to modes involving bending motions of the oxygen. The magnitudes of the isotopic shifts are consistent with assignment of these frequencies to bending modes, i.e. 3–13 cm^{-1} (Table I, footnotes *f–h*). Again, frequencies attributed to oxygen bending motions are all significantly higher than in $[TeOF_5]^-$, supporting our contention that the Xe=O bond order is substantially enhanced by the presence of a stereochemically active lone pair localized in the octahedral faces adjacent to the axial fluorine.

A ^{129}Xe Mössbauer spectrum of $Cs^+[XeOF_5]^-$ consisted of a quadrupole doublet ΔE_Q = 16.6 (1) mm s^{-1} having an isomer shift S = 0.03 (4) mm s^{-1} (relative to the $Na_6H_2{}^{129}IO_6$ source) and a line width Γ = 10.2 (1) mm s^{-1}. The quadrupole splitting shows only a slightly greater charge symmetry for $[XeOF_5]^-$ than for $XeOF_4$ (18.1 (5) mm s^{-1});[16] this is in accord with structure I. No definitive comments can be made about the very small isomer shift, which is common to all xenon compounds examined thus far.[16]

$Cs^+[(XeOF_4)_3F]^-$. X-ray Crystallography. The solid-state structure consists of Cs^+ cations and $[(XeOF_4)_3F]^-$ anions. The anions possess C_3 symmetry, which is consistent with the earlier X-ray powder data and the $^{16}O/^{18}O$ isotopic substitution experiments with their resulting vibrational coupling patterns.[13] A

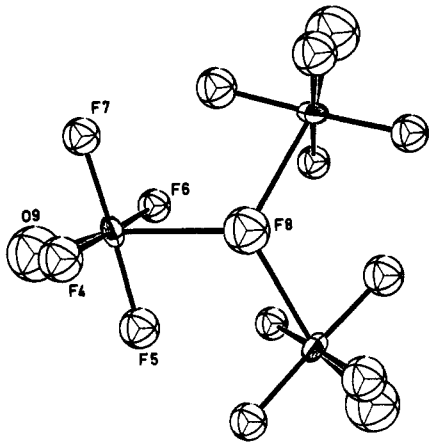

Figure 3. Structure of the $[(XeOF_4)_3F]^-$ anion with the atom-numbering scheme. The threefold axis runs through fluorine atom F(8), perpendicular to the plane of the paper.

Table II. Interatomic Distances (Å) and Angles (deg) for the $[(XeOF_4)_3F]^-$ Anion[a]

Distances			
Xe(3)–F(4)	1.94 (3)	Xe(3)–F(8)	2.62 (1)
Xe(3)–F(5)	1.92 (3)	Xe(3)–O(9)	1.70 (5)
Xe(3)–F(6)	1.89 (3)	Xe(3)···F'(5)	3.40 (3)
Xe(3)–F(7)	1.92 (3)	Xe(3)···O'(9)	3.41 (3)
Angles			
F(4)–Xe(3)–F(5)	87.0 (1.4)	F(5)–Xe(3)–O(9)	88.5 (2.4)
F(4)–Xe(3)–F(6)	177.0 (1.3)	F(6)–Xe(3)–F(7)	91.2 (1.2)
F(4)–Xe(3)–F(7)	87.3 (1.3)	F(6)–Xe(3)–F(8)	77.7 (1.6)
F(4)–Xe(3)–F(8)	105.2 (1.7)	F(6)–Xe(3)–F'(5)	60.6 (1.0)
F(4)–Xe(3)–O(9)	78.7 (2.2)	F(6)–Xe(3)–O(9)	98.8 (2.1)
F(4)–Xe(3)–O'(9)	61.0 (1.3)	F(7)–Xe(3)–F(8)	104.2 (1.0)
F(5)–Xe(3)–F(6)	94.4 (1.3)	F(7)–Xe(3)–O(9)	91.2 (2.4)
F(5)–Xe(3)–F(7)	174.3 (1.4)	F(7)–Xe(3)–F'(5)	54.8 (1.0)
F(5)–Xe(3)–F(8)	76.6 (1.0)	F(7)–Xe(3)–O'(9)	63.1 (1.3)
		F(8)–Xe(3)–O(9)	164.2 (2.3)
		F'(5)–Xe(3)–F(8)	55.0 (1.0)
		F'(5)–Xe(3)–O'(9)	61.0 (1.0)
		F(8)–Xe(3)–O'(9)	61.0 (1.3)
Xe(3)–F(8)–Xe'(3)	116.5 (0.8)		

[a] Estimated standard deviations in parentheses.

stereoscopic view of the unit cell content is shown in Figure 2 (supplementary material). The $[(XeOF_4)_3F]^-$ anion, shown in Figure 3, possesses crystallographic threefold symmetry. The xenons are six-coordinate, with five F atoms and one O atom forming a distorted octahedron about each xenon. The four atoms F(4), F(5), F(6), and F(7) lie aproximately 0.03 Å out of their least-squares plane, with F(4) and F(6) on the opposite side to

F(5) and F(7). The xenon atom is 0.02 Å out of this plane on the same side as F(5) and F(7). Table II gives selected bond lengths and angles. Four terminal Xe–F bond lengths are in the range 1.89 (3)–1.94 (3) Å, with a mean bond length of 1.90 (3) Å, compared with 1.95 (5) Å in free $XeOF_4$,[17] the value obtained from its microwave spectrum. The Xe–F bond lengths are also comparable with the values of 1.953 (2) and 2.00 (1) Å found for XeF_4[18] and XeF_2,[19] respectively. Slightly shorter terminal distances have been observed in $[XeF_5]^+[PtF_6]^-$,[20] $[XeF_5]^+[AsF_6]^-$,[21] $[XeF_5]^+[RuF_6]^-$,[22] and $[XeF_5]_2^+[PdF_6]^{2-}$[23] in which the xenon has five close fluorine atom neighbors in a square-pyramidal arrangement.

The bridging Xe---F bond length of 2.62 (1) Å is distinctly longer than the terminal ones. Nevertheless, it is clearly indicative of covalent bonding between Xe and F since it is significantly shorter than the distances of about 3.2 Å found for nonbonding xenon–fluorine contacts in XeF_4 and the van der Waals contact of 3.5 Å. In fact, the bridging bond lengths are not dissimilar from some of those in the structure of the cubic phase of XeF_6 (at 193 K).[24] The tetrameric $(XeF_6)_4$ unit has four short and four long Xe---F distances (at 2.23 (3) and 2.60 (3) Å, respectively), and the bridging bond length in $[(XeOF_4)_3F]^-$ is very close to the latter. The hexameric $(XeF_6)_6$ has three equal Xe---F contacts at 2.56 (2) Å, and here the similarity is even more striking since, not only do the bridging bond lengths differ by only 0.06 Å, but the bridging F atom is trigonally bonded and out of the plane of three associated xenon atoms in both cases. The bridging bond lengths in $[(XeOF_4)_3F]^-$ can also be compared with those in $[XeF_5]^+$ salts. For example, in $[XeF_5]^+[AsF_6]^-$[21] and $[XeF_5]^+[PtF_6]^-$,[20] the Xe---F bridging bonds in the $[PtF_6]^-$ salt are 2.52, 2.65, 2.95, and 2.95 Å (mean 2.77 Å) while in the $[XeF_5]^+[AsF_6]^-$ dimer bridging distances of 2.65, 2.73, and 2.83 Å (mean 2.73 Å) are found. Comparable bridging distances are also found in the $[RuF_6]^-$ (mean 2.75 Å)[22] and $[PdF_6]^{2-}$ (mean 2.39 Å)[23] salts. In the structure of $K^+[XeO_3F]^-$, in which XeO_3 units are linked by bridging F atoms into infinite chains, the two independent Xe---F bridging distances are shorter at 2.36 and 2.48 Å.[10]

The xenon–oxygen bond length (1.70 (5) Å) suggests considerable double-bond character and is the same as that observed in free $XeOF_4$.[17] It is a little shorter than the bond in crystalline XeO_3[25] where the Xe–O bond lengths are 1.74 (3), 1.76 (3), and 1.77 (3) Å and in crystalline $K^+[XeO_3F]^-$[10] where the distances are 1.75 (1), 1.76 (1), and 1.79 (1) Å.

The three equal bridging Xe---F---Xe angles at F(8) are 116.5 (8)°, showing that the bridging F atom and the three Xe atoms do not lie in the same plane. The distance of the F atom from the plane of the three Xe atoms is 0.49 Å. A similar arrangement of three octahedra sharing a common F atom has been found in the structure of $NaSb_3F_{10}$,[26] where three equal bridging Sb–F bonds of 2.381 (1) Å lie in the same plane. The resultant $[(SbF_3)_3F]^-$ ions are linked further through asymmetric Sb–F–Sb bonds to form infinite $[Sb_3F_{10}]_n^{n-}$ sheets. The structure of the hexameric $(XeF_6)_6$ units in the cubic phase of xenon hexafluoride[24] is also closely related to that of $[(XeOF_4)_3F]^-$. In the anion three $XeOF_4$ units, which have a near-square-pyramidal structure (the average F′–Xe–F angle is 89.3°), are linked through three equivalent Xe---F bonds to a common fluorine. In $(XeF_6)_6$ three square-pyramidal $[XeF_5]^+$ units have equal Xe---F bonds to a common F^-. In both cases the bridging fluorine is out of the plane of the three associated fluorine atoms. In the $(XeF_6)_6$ structure (and in the related $[XeF_5]^+[AsF_6]^-$[21] and $[XeF_5]_2^+[PdF_6]^{2-}$[23] structures) each xenon is linked to three bridging fluorines trigonally disposed below the base of the square-pyramidal $[XeF_5]^+$ cation. An outstanding feature of this arrangement is that the three bridging fluoride ions are not close to the fourfold axis of the $[XeF_5]^+$ cation. A similar feature exists in $[XeF_5]^+[PtF_6]^-$ and $[XeF_5]^+[RuF_6]^-$ in which the xenon atom is similarly bonded to four bridging fluorines, which also avoid the fourfold axis of the $[XeF_5]^+$ cation. This is consistent with the nonbonding electron pair being on the fourfold axis. In the $[(XeOF_4)_3F]^-$ case only one bridging bond emanates from the base of the $XeOF_4$ square pyramid. This bond bisects the F(6),Xe,F(5) plane, i.e. ∠(F(5)–Xe–F(8)) = 77° and ∠(F(6)–Xe–F(8)) = 78° (Table III), and subtends an angle of 71° with the plane. The bridge bond also bisects the F(7),Xe,F(4) plane, and the angle from the plane is 111°.

Table III. Some Significant Contact Distances (Å) and Contact Angles (deg) for Xenon in the $[(XeOF_4)_3F]^-$ Anion[a]

	Distances		
Xe(3)–F(8)	2.62 (1)	Xe(3)–O′(9)	3.41 (6)
Xe(3)–F′(5)	3.40 (3)		
	Angles		
	Part A		
F(5)–Xe(3)–F(8)	76.6 (1.3)	F(6)–Xe(3)–F(8)	77.7 (1.1)
F(4)–Xe(3)–O′(9)	61.0 (1.3)	F(6)–Xe(3)–F′(5)	60.6 (1.0)
F(7)–Xe(3)–O′(9)	63.1 (1.3)	F(7)–Xe(3)–F′(5)	54.8 (1.0)
	Part B		
F′(5)–Xe(3)–F(8)	55.0 (1.0)	F(8)–Xe(3)–O′(9)	61.0 (1.3)
F′(5)–Xe(3)–O′(9)	61.0 (1.0)		

[a] Estimated standard deviation in parentheses.

In addition, there are two further long contacts, secondary bonds with xenon, one involving an oxygen (O′(9)) at 3.41 (6) Å and another involving a fluorine (F′(5)) at 3.40 (3) Å (Table III). The angles subtended by these additional long contacts with xenon and their nearest-neighbor Xe–F bonds are also given in Table III (Part A) and indicate that the O′(9) contact with Xe bisects the plane F(4),Xe,F(7) and the F′(5) contact with Xe bisects the plane F(6),Xe,F(7). The angles between the long contacts (Table III, part B) show a near-regular trigonal arrangement for the contacting atoms below the XeF_4 plane (Figure 4; supplementary material). This arrangement is similar to the trigonal arrangement of Xe---F interactions noted earlier in this discussion in the structures of $(XeF_6)_6$, $[XeF_5]^+[AsF_6]^-$, and $[XeF_5]_2^+[PdF_6]^{2-}$ in which the bridging atoms avoid the fourfold axis of $[XeF_5]^+$. It appears that the stereochemically active lone pair of xenon is either located between the contacting F(8), F′(5), and O′(9) atoms close to the fourfold axis of $XeOF_4$ or in the greater spatial void afforded beneath the F(4),Xe,F(5) plane, with its projection on the plane approximately bisecting ∠F(4),Xe,F(5) (Figure 4). The angles between the long contacts and their respective planes are 50° for O′(9)---Xe and plane F(4),Xe,F(7) and 40° for F′(5)---Xe and plane F(6),Xe,F(7). The secondary bonds may be regarded as passing through three of the four octahedral faces defined by the XeF_4 plane and an extension of the fourfold axis beneath this plane. Alternatively then, the fourth vacant octahedral face beneath plane F(4),Xe,F(5) could accommodate the stereochemically active xenon lone pair.

The cesium ions lie on threefold crystallographic axes and form 12 nonbonded contacts with the fluorine atoms. Cs(1) is coordinated to six F(5) atoms at 3.23 (3) Å and six F(7) atoms at 3.08 (3) Å, while Cs(2) is coordinated with six F(4) atoms at 3.15 (3) Å and six F(6) atoms at 3.18 (3) Å.

Raman Spectroscopy. The crystal structure shows that $[(XeOF_4)_3F]^-$ possesses C_3 symmetry and should therefore exhibit 51 normal modes of vibration, $\Gamma = 17\ A_1 + 17\ E$, where the A and E modes are Raman and infrared active, giving a total of 34

(17) Martins, J.; Wilson, E. B. *J. Chem. Phys.* **1964**, *41*, 570.
(18) Burns, J. H.; Agron, P. A.; Levy, H. A. *Science* (Washington, D.C.) **1963**, *No. 139*, 1208.
(19) Levy, H. A.; Agron, P. A. *J. Am. Chem. Soc.* **1963**, *85*, 241.
(20) Bartlett, N.; Einstein, F.; Stewart, D. F.; Trotter, J. *J. Chem. Soc. A* **1967**, 1190.
(21) Bartlett, N.; DeBoer, B. G.; Hollander, F. J.; Sladky, F. O.; Templeton, D. H.; Zalkin, A. *Inorg. Chem.* **1974**, *13*, 780.
(22) Bartlett, N.; Gennis, M.; Gibler, D. D.; Morrell, B. K.; Zalkin, A. *Inorg. Chem.* **1973**, *12*, 1717.
(23) Leary, J.; Templeton, D. H.; Zalkin, A.; Bartlett, N. *Inorg. Chem.* **1973**, *12*, 1726.
(24) Burbank, R. D.; Jones, G. R. *J. Am. Chem. Soc.* **1974**, *96*, 43.
(25) Templeton, D.; Zalkin, H. A.; Forrester, J. D.; Williamson, S. M. *J. Am. Chem. Soc.* **1963**, *85*, 817.
(26) Fourcade, F.; Mascherpa, G.; Philippot, E. *Acta Crystallogr., Sect. B: Struct. Crystallogr. Cryst. Chem.* **1975**, *B31*, 2322.

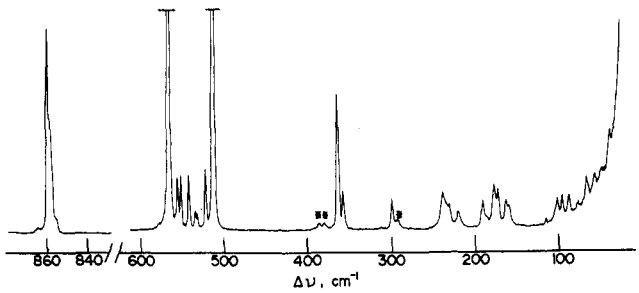

Figure 5. Raman spectrum of 99% ^{18}O-enriched $Cs^+[(XeOF_4)_3F]^-$ recorded at −196 °C (asterisks denote FEP sample vessel lines).

Table IV. Raman Spectra and Assignments for $[(XeOF_4)_3F]^-$ and $XeOF_4$

$Cs^+[(XeOF_4)_3F]^-$	$XeOF_4$[a]	assgnt and approx descr, C_{4v} sym
905 (41)[b]	919 s	a_1, ν(Xe=O)
566 (100), 556 (3)	609 vs[f]	e, $\nu_{asym}(XeF_4)$
551 (3), 542 (3)	566 vs	a_1, $\nu_{sym}(XeF_4)$
534 (1), 532 (1), 521 (4), 511 (46)	530 w	b_1, $\nu_{sym}(XeF_4)$ out-of-plane
476 (8), 362 (8)[d,e]	364 mw	e, $\delta(F_4Xe{=}O)$
300 (2), 292 (1)[e]	286 vw	a_1, $\delta_{sym}(XeF_4)$ out-of-plane
238 (2), 231 (1)[e]	231 s	b_1, $\delta_{sym}(XeF_4)$ in plane
220 (1)		
191 (1.5), 187 (0.5)[e]	not obsd	b_2, $\delta_{asym}(XeF_4)$ out-of-plane
178 (2), 173 (2)[e]		
163 (2), 160 (1)[e]	161 vw	e, $\delta_{asym}(XeF_4)$ in plane
115 (0.5), 101 (1), 96 (1), 87 (1), 76 (0.5), 66 (2), 56 (1), 48 (0.5), 38 (2)		lattice modes

[a] References 28 and 29. [b] $^{16}O/^{18}O$ isotopic shift: 45 cm^{-1}. [c] Vibrationally coupled Xe-F stretching modes. [d] $^{16}O/^{18}O$ isotopic shift: 14 cm^{-1} (see Figure 6A,B). [e] Represent the a_1 (high-frequency line) and e (low-frequency line) components due to vibrational coupling under C_3 symmetry. [f] Not observed in the Raman spectrum; value obtained from the infrared spectrum.

Raman-active bands. A factor-group analysis[27] shows that, when the normal vibrational modes of the free anion (C_3) are correlated to the crystal site symmetry (C_3) and, in turn, to the unit cell symmetry (T_h), each vibrational mode of the free ion should be split, giving $\Gamma = 34\ A_g + 34\ E_g + 34\ F_g + 34\ A_u + 34\ E_u + 34\ F_u$, where A_g, E_g, and F_g are Raman active and E_u is infrared active. Thus, the Raman spectrum of the anion, strongly coupled both intramolecularly and in the unit cell, should display a maximum of 102 Raman-active vibrational bands. Clearly, coupling within the unit cell of $Cs^+[(XeOF_4)_3]^-$ is weak and cannot be resolved. It is apparent that intramolecular coupling among the three molecules of $XeOF_4$ bridged to a common fluoride ion is also not resolved in all cases. In fact, only 22 (plus nine lattice modes) of the maximum of 34 vibrational bands expected in the absence of factor-group splitting are resolved in the low-temperature Raman spectrum (Figure 5). The assignments of the $XeOF_4$ group modes of $[(XeOF_4)_3F]^-$ have been made by comparison with the corresponding previously assigned modes for $XeOF_4$ (C_{4v})[28,29] and are consequently listed under C_{4v} symmetry in Table IV.

The presence of a single, sharp Xe=O stretching mode at 905 cm^{-1} (^{16}O compound) and 860 cm^{-1} (^{18}O compound) and only two bands at 905 and 860 cm^{-1} in the 61.9% ^{18}O-enriched compound in the ratio 2:3 is consistent with all three coordinated $XeOF_4$ molecules being equivalently bonded to a central fluoride ion. Apparently, vibrational coupling among the individual Xe=O stretching modes in the anion is extremely weak and does not lead to splitting of these lines in the natural-abundance or 99% ^{18}O-enriched compounds; nor does it permit the resolution of the individual in-phase and out-of-phase Xe=O stretching modes arising from $[(Xe^{18}OF_4)_2(Xe^{16}OF_4)F]^-$ and $[(Xe^{18}OF_4)(Xe^{16}OF_4)_2F]^-$. The Xe=O stretching mode in the anion is only marginally lower in frequency than that in $XeOF_4$, but substantially higher than that in $[XeOF_5]^-$, reflecting the low net negative charge associated with each $XeOF_4$ in $[(XeOF_4)_3F]^-$.

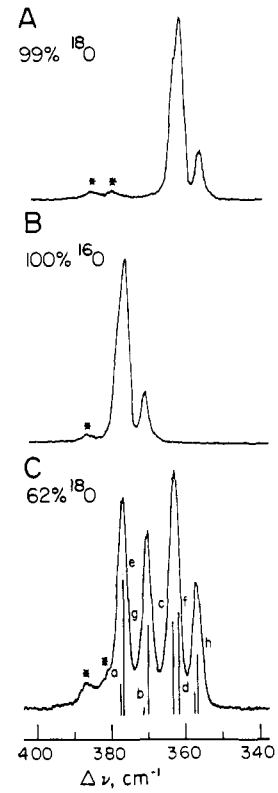

Figure 6. Vibrationally coupled $F_4Xe{=}O$ bends of the $[(XeOF_4)_3F]^-$ anion (recorded at −196 °C): (A) 99% ^{18}O enriched; (B) 100% ^{16}O; (C) 61.9% ^{18}O enriched, where a, b, and c represent A and E modes of $[(Xe^{16}OF_4)_3F]^-$ and $[(Xe^{18}OF_4)_3F]^-$, respectively, under C_3 symmetry and e,f and g,h represent A′ modes of $[(Xe^{16}OF_4)_2(Xe^{18}OF_4)F]^-$ and $[(Xe^{16}OF_4)(Xe^{18}OF_4)_2F]^-$, respectively, under C_s symmetry.

Those bands not exhibiting an $^{18}O/^{16}O$ dependence have been assigned to XeF_4 group stretching and bending modes. In contrast to the Xe=O stretching modes, these modes are extensively coupled, yielding, in the case of the stretching modes, severely overlapping patterns of bands that cannot be assigned in detail by analogy with $XeOF_4$. Consequently, only tentative assignments of the coupled lines are given in Table IV.

Other than the Xe=O stretch at 905 cm^{-1}, the only vibrational modes in $[(XeOF_4)_3F]^-$ involving oxygen motions that exhibit a substantial $^{16}O/^{18}O$ isotopic dependence are the $F_4Xe{=}O$ bends. Unlike the Xe=O stretch, however, these modes are also strongly coupled. A detailed consideration of the strong vibrational coupling among $F_4Xe{=}^{16}O$ and $F_4Xe{=}^{18}O$ bending modes in the anion confirms that the three $XeOF_4$ molecules are equivalently bonded to the central fluorine atom. The easily resolved A and E components (under C_3 symmetry), which result from coupling of these bends, have the expected identical relative intensities in both the ^{16}O and ^{18}O compounds and possess a substantial isotopic shift of 14 cm^{-1} (Figure 6A,B). Intermediate levels of ^{18}O enrichment resulted in statistical mixtures of all possible isotopic isomers, i.e. the two C_{3v} species $[(Xe^{16}OF_4)_3F]^-$ and $[(Xe^{18}OF_4)_3]^-$ discussed above and the two C_s species $[(Xe^{16}OF_4)_2(Xe^{18}OF_4)F]^-$ and $[(Xe^{16}OF_4)(Xe^{18}OF_4)_2F]^-$. The calculated percentage abundances of the isomers at 61.9% ^{18}O enrichment are 5.5, 23.7, 27.0, and 43.8%, respectively. Reduction of C_3 symmetry to C_s

(27) Fateley, W. G.; Dollish, F. R.; McDevitt, N. T.; Bentley, F. F. "Infrared and Raman Selection Rules for Molecular and Lattice Vibrations: The Correlation Method"; Wiley-Interscience: New York, 1972.
(28) Claassen, H. H.; Chernick, C. L.; Malm, J. G. In "Noble-Gas Compounds"; Hyman, H. H., Ed.; University of Chicago Press: Chicago IL, 1963; p 287.
(29) Begun, G. M.; Fletcher, W. H.; Smith, D. F. *J. Chem. Phys.* **1965**, *42*, 2236.

symmetry in the latter two isomers results in splitting of the asymmetrically coupled $F_4Xe{=}O$ bends belonging to the E-symmetry species into their respective A′ and A″ components in each of the two C_s isomers. The spectrum and overlap scheme for the A, E, and A′ modes resulting from vibrational coupling of the $F_4Xe{=}O$ bends in statistical mixtures of the four isotopic isomers at 61.9% ^{18}O enrichment are depicted in Figure 6C. The asymmetric A″ components are expected to be considerably less intense than the symmetric A′ component. Thus, the two A″ modes arising from $[(Xe^{16}OF_4)_2(Xe^{18}OF_4)F]^-$ and from $[(Xe^{16}OF_4)(Xe^{18}OF_4)_2F]^-$ are not included in the splitting scheme (Figure 6C) owing to their apparent low intensities and extensive overlap with other more intense $F_4Xe{=}O$ bends in this region of the spectrum.

It has not been possible to assign the two anticipated bands arising from xenon-bridging fluorine symmetric and asymmetric stretches. Both these frequencies would presumably occur below 400 cm^{-1} (cf. $Xe_2F_3^+$ and XeF^+ compounds in ref 7) and be very weak.

Experimental Section

Apparatus and Materials. All manipulations involving air-sensitive materials were carried out under anhydrous conditions on vacuum lines constructed from 316 stainless-steel, nickel, Teflon, and FEP and/or in a drybox. Xenon hexafluoride and $XeOF_4$ were transferred under vacuum through FEP and Teflon connections previously passivated with fluorine. Air-sensitive or previously dried substances of low volatility, i.e., CsF, NaF, $Cs^+[XeOF_5]^-$, and $Cs^+[(XeOF_4)_3F]^-$, were transferred in a drybox. All preparative work was carried out in $^1/_4$-in. o.d. lengths of FEP tubing heat sealed at one end and connected through 45° SAE flares to custom-built Kel-F valves or by compression unions to Teflon valves (Production Techniques, Ltd.).

Xenon hexafluoride was prepared from xenon (Linde, CP grade or British Oxygen Corp.) and fluorine (Air Products or Matheson) according to the method described by Malm and Chernick.[30] Natural-abundance and ^{18}O-enriched water (61.9% and 99%, Prochem) were used in the preparations of $XeOF_4$ from XeF_6. Pure liquid samples of $XeOF_4$ were made by the direct combination of water vapor with XeF_6[31] previously condensed in an evacuated, passivated 2-L valved nickel reaction vessel (6-mm walls). Prior to use, the walls of the vessel were reduced a total of three times at ~400 °C with 5 atm (25 °C) of H_2 pressure for 1 h and pumped out while still hot. This was done to ensure removal of ^{16}O oxide, which might exchange with $XeOF_4$ and/or react with XeF_6, diluting the ^{18}O preparations. Subsequent to reduction, the vessel was heated to red heat in the presence of 2 atm (25 °C) of F_2 gas (repeated three times), cooled, and evacuated. Approximately 1 g of XeF_6 was condensed into the vessel and its vapor allowed to remain in contact with the vessel walls for at least 1 day before being pumped out and discarded. In typical preparations, 1.69 mmol of ^{18}O-enriched H_2O was condensed at −169 °C onto the vessel walls above XeF_6 (1.69 mmol). The vessel was allowed to warm slowly to room temperature [*Caution*! danger of explosion] and stand for 4 h before being agitated. The vessel was allowed to remain at room temperature for another 8 h before the products, HF, $XeOF_4$, and an excess of XeF_6, were vacuum distilled into a Kel-F tube containing NaF (previously dried under vacuum at 300 °C for 24 h). Pure $XeOF_4$ of the desired oxygen isotope enrichment was distilled from the appropriate storage vessel as required.

$Cs^+[(XeOF_4)_3F]^-$. An excess of $XeOF_4$ was vacuum distilled onto CsF (dried at 350 °C under vacuum for $1^1/_2$ days). In a typical preparation, an excess of $XeOF_4$ (~3.0 g) was allowed to remain in contact with CsF (0.3184 g, 2.096 mmol). As the reaction progressed, the volume of undissolved white solid was noted to increase substantially. After 2 days, unreacted $XeOF_4$ was removed at 0 °C by static distillation into an FEP vessel cooled to −196 °C. After 1 h, no substantial change in mass of the resulting white solid could be detected, yielding a total mass of 1.3684 g for the product, which corresponded to the stoichiometry $CsF{\cdot}2.93XeOF_4$.

$Cs^+[XeOF_5]^-$. The preparation of $Cs^+[XeOF_5]^-$ was identical, except that the excess of $XeOF_4$ was removed by dynamic vacuum distillation at room temperature. In a typical preparation, the sample of $Cs^+[(XeOF_4)_3F]^-$ described above was pumped on at room temperature. A weight loss vs. time pumping curve at room temperature revealed that the minimum weight was reached within 1 h, yielding the composition $CsF{\cdot}0.995XeOF_4$.

Table V. Fractional Atomic Coordinates (×10⁴) for $Cs[(XeOF_4)_3F]$[a]

atom	x	y	z
Cs(1)	0	0	0
Cs(2)	5000	5000	5000
Xe(3)	2460 (2)	2548 (2)	4768 (2)
F(4)	1748 (23)	1368 (23)	4574 (25)
F(5)	3603 (24)	1802 (23)	4593 (24)
F(6)	3124 (19)	3700 (19)	5021 (18)
F(7)	1248 (22)	3182 (20)	4905 (21)
F(8)	3054 (26)	3054 (26)	3054 (26)
O(9)	2393 (47)	2118 (37)	5908 (38)

[a] Estimated standard deviations in parentheses.

Crystal Data: $CsF_{13}O_3Xe_3$, M_r = 821.81, cubic, space group *Pa*3 (No. 205), a = 13.933 (7) Å, V = 2704.8 Å³, Z = 8, D_{calcd} = 4.035 g cm^{-3}, F(000) = 2864, μ(Mo Kα) = 96.3 cm^{-1}, λ(Mo Kα_1) = 0.709 26 A, λ(Mo Kα_2) = 0.713 54 Å, mean 0.7107 Å). suitable crystals for X-ray work were grown by the slow concentration of solutions of CsF in $XeOF_4$ in near-horizontal 1.9-cm Kel-F tubes. When well-formed crystals were apparent in the tubes, the excess of solution was decanted off, the tubes were evacuated, and dry nitrogen was admitted. The crystals were colorless cubes and were transferred into prefluorinated Teflon-FEP capillaries in a nitrogen-filled drybox.

X-ray Data Collection. Preliminary Weissenberg and precision photographs showed that the crystals were generally of poor quality with multiple components and decomposed rapidly with time and/or irradiation. The crystal used for data collection, of approximate dimensions 0.22 × 0.32 × 0.42 mm^3, was mounted with one of the cubic axes coincident with the ω axis of the Stoe Stadi-2 Weissenberg diffractometer. The lattice parameter a was determined from the position of 20 high-angle (α_1, α_2) resolved reflections ($2\theta > 48°$). The positions of both α_1 and α_2 components were obtained by fitting $\theta/2\theta$ diffraction scan profiles to two overlapping Gaussian functions. The intensities of a full half-sphere of reflections, with $0.08 < (\sin\theta)/\lambda < 0.64$ Å^{-1} were measured by using a ω-scan technique (2.4° min^{-1}) at 293 (1) K with graphite-monochromated Mo Kα radiation. The crystal deteriorated to approximately 65% of its original scattering power during the data collection. After corrections for crystal decomposition, Lorentz, polarization, and absorption effects (transmission factors from 0.1597 to 0.0456), 2435 reflections have $I > 3\sigma(I)$ were averaged to 355 unique reflections ($R_{internal}$ = 0.24).

Structure Solution and Refinement. The structure was solved by conventional heavy-atom methods and refined by the full-matrix least-squares method. At this stage, although a well-defined structure with sensible thermal parameters had been obtained, the R factor remained high (~0.15). An F_o/F_c analysis of the individual measurements of each unique reflection, many of which were measured 12 times, showed that some intensities of a given set were much higher than the remainder, which were much closer to the calculated value. Since diffraction photographs of the data crystal showed the presence of several other misaligned fragments, it was assumed that the higher than expected intensity measurements arose from chance coincidences with reflections from these other components. Some 274 of the worst such measurements were removed from the total data set, and after remerging, the structure refinement was continued. Although the $R_{internal}$ remained high (0.17), there were many fewer bad inconsistencies. In the final refinement cycle, with anisotropic thermal parameters for the Cs and Xe atoms and isotropic parameters for F and O, R = 0.0969 and R_w = 0.0960 for 355 unique reflections and 36 parameters. The function minimized was $\sum w||F_o| - |F_c||^2$ with $w = 1.289/[\sigma^2(F_o) + 0.014F_o^2]$; the weighting scheme over $|F_o|$ and $(\sin\theta)/\lambda$ showed no systematic trends. No evidence of extinction effects in the data could be detected. A final difference Fourier map contained maximum peaks at approximately 5 e Å^{-3} close to the xenon atoms. The SHELX 76[32] program was used in all calculations. Scattering factors for neutral atoms were taken from ref 33 and were corrected for anomalous dispersion. The final atomic positional parameters are given in Table V, and bond lengths, bond angles, and some significant contact distances and contact angles are given in Tables II and III, respectively. Final structure factor tables and a listing of anisotropic thermal parameters have been deposited as supplementary material.

Laser Raman Spectroscopy. A Spectra-Physics Model 164 argon ion laser giving up to 900 mW at 5145 Å was used to excite the Raman

(30) Chernick, C. L.; Malm, J. G. *Inorg. Synth.* **1966**, *8*, 258.
(31) Chernick, C. L.; Claassen, H. H.; Malm, J. G.; Plurien, P. L.; In ref 28, p 106.
(32) Sheldrick, G. M. "SHELX, Program for Crystal Structure Determination"; University of Cambridge: Cambridge, England, 1976.
(33) "International Tables for X-Ray Crystallography"; Kynoch Press: Birmingham, England, 1974; Vol. 4, pp 99–100, 149–150.

spectra. The spectrometer was a Spex Industries Model 14018 double monochromator equipped with 1800-grooves/mm holographic gratings. An RCA C31034 phototube detector in conjunction with a pulse count system consisting of pulse amplifier, analyzer, and rate meter (Hamner NA-11, NC-11, and N-78A, respectively) and a Texas Instruments Model FSOZWBA strip chart recorder were used to record the spectra. The spectrometer was periodically calibrated by recording the discharge lines from an argon lamp over the spectral range of interest; the Raman shifts quoted are estimated to be accurate to ±1 cm^{-1}. Slit widths depended on the scattering efficiency of the sample, laser power, etc., with 1.0 cm^{-1} being typical.

FEP reaction vessels were mounted vertically. The angle between the incident laser beam and the sample tube was 45°, and Raman scattered radiation was observed at 45° to the laser beam (90° to the sample tube axis).

All spectra were recorded at −196 °C by mounting the sample vertically in an unsilvered Pyrex glass Dewar filled with liquid nitrogen.

Acknowledgment. We thank the Science and Engineering Research Council of Great Britain (J.H.H.) and the Natural Sciences and Engineering Research Council of Canada (G.J.S.) for financial support of this work, NATO for travel grants (D.M.-R. and G.J.S.), and the University of Leicester Computer Laboratory for use of their facilities. H.S. and V.K. were on leave from the Hebrew University of Jerusalem, Israel, and Edvard Kardelj University of Ljubljana, Yugoslavia, respectively. We also thank Prof. Hendrik de Waard, Laboratorium voor Algemene Natuurkunde, University of Groningen, The Netherlands, for obtaining the ^{129}Xe Mössbauer data on $Cs^+[XeOF_5]^-$.

Registry No. $Cs^+[(XeOF_4)_3F]^-$, 76077-76-4; $XeOF_4$, 13774-85-1; $Cs^+[XeOF_5]^-$, 12191-01-4; ^{18}O, 14797-71-8.

Supplementary Material Available: Listings of thermal parameters, observed and calculated structure factors, and details of least-squares planes and Figures 2 and 4 showing a stereoscopic view of the unit cell and a view down the fourfold axis of one $XeOF_4$ group in $Cs^+[(XeOF_4)_3F]^-$, respectively (7 pages). Ordering information is given on any current masthead page.

Contribution from the Institut für Anorganische Chemie, Technische Universität München, D-8046 Garching, West Germany, and Institut für Anorganische Chemie der Rheinisch-Westfälischen Technischen Hochschule Aachen, D-5100 Aachen, West Germany

Antiferromagnetic Coupling of Cobalt (d^9) Centers Mediated by the Norbornadiene π Systems

HANS-F. KLEIN,*[†,‡] LASZLO FABRY,[†] HUBERT WITTY,[‡] ULRICH SCHUBERT,[‡,§] HEIKO LUEKEN,[∥] and ULRICH STAMM[∥]

Received March 9, 1984

The synthesis and properties of cobalt(0) complexes with bicyclo[2.2.1]heptadiene, $Co(C_7H_8)(PMe_3)_3$ and $C_7H_8[Co(PMe_3)_3]_2$, and with bicyclo[2.2.1]heptene, $Co(C_7H_{10})(PMe_3)_3$, are reported. The X-ray structure investigation of the binuclear exo/exo metal complex with the norbornadiene bridge shows that it crystallizes in the monoclinic space group $C2/c$, with a = 15.743 (4) Å, b = 9.291 (3) Å, c = 28.777 (9) Å, β = 116.94 (2)°, and Z = 4. The structure shows isolated molecular units with each cobalt tetrahedrally surrounded by three phosphane ligands and one olefinic function. From magnetic susceptibility data, a remarkably strong antiferromagnetic coupling of the d^9 centers (d_{Co-Co} = 5.749 (1) Å) involving through-space interactions between the norbornadiene π systems is found (singlet–triplet splitting $\Delta E = E(T) - E(S) \approx 500$ cm^{-1}).

Introduction

Zerovalent cobalt forms mononuclear complexes of composition $Co(olefin)(PMe_3)_3$.[1-3] Complexes of $Co(olefin)_2(PMe_3)_2$ can be synthesized by using diolefin ligands with isolated double bonds, provided chelating effects enhance the thermal stability of such systems.[3] We found bicyclo[2.2.1]heptadiene reacting with cobalt(0) centers not in this fashion but forming mono-exo and bis-exo complexes **1** and **2**.

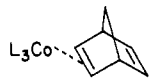

1

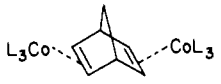

2

There has been considerable interest in π-orbital interactions in oligocyclic unsaturated molecules.[4-6] Serving as ligands for two or more paramagnetic metal centers, these molecules are expected to transmit unpaired electron density, thereby mediating spin–spin coupling between valence shells of metal centers. We therefore set out to determine the crystal structure and to investigate the magnetic properties of complex **2**.

Experimental Section

Methods and Analyses. Standard high-vacuum techniques were used in handling volatile and air-sensitive material.[7] Combustion analyses were carried out by W. Barth, U. Graf, and G. Schuller in the Garching microanalytical laboratory. Trimethylphosphine was prepared from triphenyl phosphite and methylmagnesium chloride.[8] Norbornadiene (reagent grade; Merck-Schuchardt) was distilled before use. ESR spectra were obtained at 77 K (toluene glass) on a Varian E 3 spectrometer with diphenylpicrylhydrazyl as an external standard. ^1H NMR spectra (300 MHz) were recorded on a Bruker WM 300 spectrometer equipped with a low-temperature unit.[9] Chemical shifts are referenced to internal $C_6D_5CD_2H$ (δ = 2.03). No corrections were made.

Preparations and Reactions. (Bicyclo[2.2.1]heptadiene)bis[tris(trimethylphosphine)cobalt] (2). Method a. Anhydrous cobalt chloride (1.07 g, 8.2 mmol), trimethylphosphine (2.4 mL, 24.6 mmol), and norbornadiene (0.42 mL, 4.1 mmol) in 40 mL of tetrahydrofuran were reacted with 1 g of magnesium turnings (excess). Two hours after the start of the reaction, the reddish brown solution was evaporated to dryness. The residue was extracted with three 10-mL portions of pentane. Crystallization at −78 °C gave dark red crystals (2.09 g, 77%) that

[†] Present address: Anorganisch-chemisches Institut der Technischen Hochschule, D-6100 Darmstadt, West Germany.
[‡] Technische Universität München.
[§] Present address: Institut für Anorganische Chemie der Universität Würzburg, D-8700 Würzburg, West Germany.
[∥] Technische Hochschule Aachen.

(1) Klein, H.-F.; Hammer, R.; Wenninger, J.; Gross, J. In "Catalysis in Chemistry and Biochemistry"; Pullman, B., Ed.; D. Reidel: Amsterdam, 1979; pp 285–292.
(2) Klein, H.-F. *Angew. Chem., Int. Ed. Engl.* **1980**, *19*, 362.
(3) Klein, H.-F.; Witty, H.; Neugebauer, D. *Z. Naturforsch., B: Anorg. Chem., Org. Chem.* **1984**, *39B*, 643.
(4) (a) Walsh, T. D. *J. Am. Chem. Soc.* **1969**, *91*, 515. (b) Turro, N. J.; Tobin, M.; Friedman, L.; Hamilton, J. B. *J. Am. Chem. Soc.* **1969**, *91*, 516.
(5) Hoffmann, R. *Acc. Chem. Res.* **1971**, *4*, 1.
(6) Haselbach, E.; Neuhaus, L.; Johnson, R. P.; Houk, K. N.; Paddon-Row, M. N. *Helv. Chim. Acta* **1982**, *65*, 1743.
(7) Klein, H.-F.; Karsch, H. H. *Inorg. Chem.* **1975**, *14*, 437.
(8) Wolfsberger, W.; Schmidbaur, H. *Synth. React. Inorg. Met.-Org. Chem.* **1974**, *4*, 149.
(9) We thank Dr. S. Braun, Organic Chemistry Institute, TH Darmstadt, for running the spectra.

0020-1669/85/1324-0683$01.50/0